Undersampled-based Modulation Schemes for Optical Camera Communications

Pengfei Luo, Min Zhang, Zabih Ghassemlooy, Stanislav Zvanovec, Shulan Feng, and Philipp Zhang

***Abstract*—Widespread use of white light-emitting diodes and ubiquitous smart devices offer the opportunity to establish visible light communications (VLC) which has become a hot research topic based on the growing number of publications over the last decade. Camera-based VLC, namely optical camera communications (OCC), provide many unique features when compared with a single photodiode-based system, such as the ability to separate incident light in spatial and color domains. OCC technology represents a promising approach to utilize the benefits of VLC in beyond-5G scenarios and is one of the key technologies of the Internet of Things. Establishing a long communication channel in OCC, as well as non-flickering illumination in using low-frame-rate camera detectors, requires special modulation schemes. This article provides an overview of the principles of three categories of modulation schemes for OCC systems using a low-frame-rate camera detector. In addition, a series of undersampled modulation schemes are proposed and discussed to achieve flicker-free OCC with higher spectral efficiency. In addition, framing structures are designed to solve problems occurring in OCC systems using particular modulation schemes. To evaluate the performance of these modulation schemes, measured bit error rate values are shown. Finally, challenges in the implementation of OCC systems are also outlined.**

***Index Terms* — optical camera communications, non-flickering illumination, undersampled phase shift ON-OFF keying, undersampled quadrature-amplitude-modulation, visible light communications, optical wireless communications**

I. Introduction

NOWADAYS, we are witness to the ever-increasing utilization of cameras in smart devices, vehicles, highways and roadside infrastructures. These cameras capture images, video and have the potential to receive visible light communication (VLC) signals. Optical camera communications (OCC) technology employs a camera to view and capture data from light-emitting diode (LED) based lighting fixtures that offer new possibilities for deploying VLC in several unique applications [1]. Normally, VLC systems employ a small (10^{-3}–10^{2} mm^2), high-speed (>100 MHz) non-imaging device (e.g., a photodiode (PD)) as the receiver. In single PD-based VLC systems, optical concentrators are adopted to increase the received optical power and establish a practical transmission span *d* (i.e., a few meters). However, using optical concentrators results in a sharply reduced field-of-view (FOV) of the receiver since any mismatch between the light source and the receiver might lead to signal strength variation or even loss of signal, thus limiting the practical application of VLC.

In an OCC system, a camera, composed of an imaging lens and image sensor (IS), is adopted as the receiver [2]. The camera-based receiver offers many unique features compared with the single PD-based system using an optical concentrator. For example: (*i*) a larger FOV – the IS consists of an array of PDs (pixels) which increases the angle of incidence; (*ii*) spatial separation of light - light incidents from many directions is captured by different pixels, leading to a much higher signal-to-noise ratio (SNR); and (*iii*) wavelength separation of light - in color cameras, the red, green and blue (RGB) filter array (Bayer filter) above each pixel separates the light of different wavelengths. Regarding the speed of both VLC systems, the single PD-based VLC system can support a data rate of up to several Gbps. However, due to the limitation of the sampling rate of a low-frame-rate (LFR) camera (e.g., ≤ 60 fps), the data rate of OCC is in the range of 10 bps – 100 kbps which is sufficient for a number of applications including vehicle-to-vehicle (V2V) communications [1].

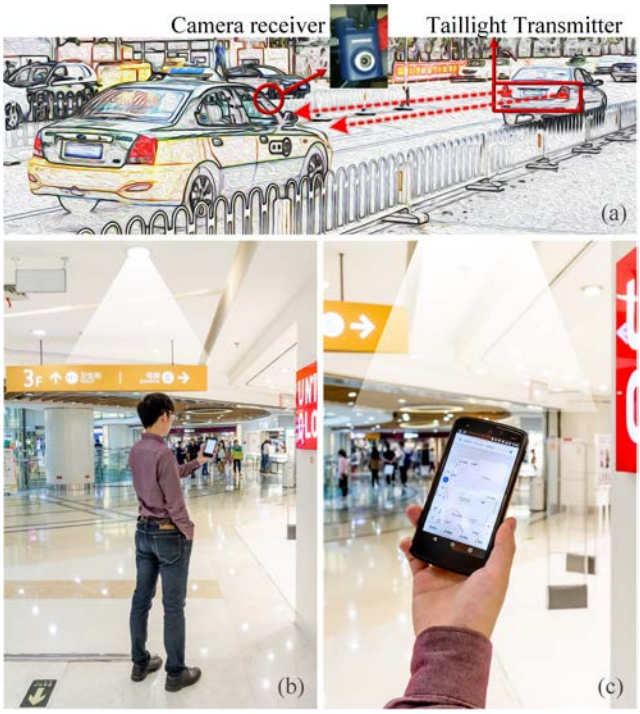

Fig. 1. Scenarios for OCC: (a) V2V communications; (b) indoor positioning; and (c) indoor mapping with real-time location of the user.

This work was supported in part by the EU cLINK project (GN. 372242-1-2012-1-UK-ERA), EU COST Action IC 1101, NSFC Project (61372119), the Royal Society Newton International Exchanges (NI140188) between UK and China, and CTU project SGS17/182/OHK3/3T/13.

Pengfei Luo, Shulan Feng and Philipp Zhang are with Huawei Technologies Co., Ltd;

Min Zhang is with Beijing University of Posts and Telecommunications; Zabih Ghassemlooy is with Northumbria University; Stanislav Zvanovec is with Czech Technical University in Prague.

OCC technology could be used in many scenarios, especially in conjunction with other wireless communication technologies, such as V2V communications (see Fig. 1(a)), where vehicles could exchange real-time, safety-related traffic information (e.g., accident notifications, braking performance, speed, and direction). In this scenario, the received information may then be uploaded to the cloud through the cellular network to help other road users [2]. Another scenario involves retailing where LED-based ceiling lights in stores transmit site maps or information related to products, and how to locate them, to the smart devices of customers (see Figs. 1(b) and (c)). Such a system can receive positioning beacon signals from the lighting infrastructure. By integrating detection and positioning algorithms, OCC can offer highly accurate indoor and urban canyon positioning which is difficult to achieve with other existing positioning technologies [3, 4].

Since the frame rate R_{fc} of a commercial camera is typically low (e.g., 25–50 fps), on-off keying (OOK) will introduce flickering. To provide flicker-free lighting, the flickering frequency f_{fl} must be higher than the critical flicker frequency (CFF) f_{cf} of the human eye (i.e., ~100 Hz [5]). For these purposes, an LFR camera is too slow to receive signals. To overcome this problem, dedicated modulation schemes have been proposed.

This article introduces the concept, characteristics and advantages of OCC technology. A review of the various types of OCC systems and modulation schemes follows. Next, we focus on undersampled-based modulation schemes. Corresponding data framing strategies are subsequently introduced to facilitate the implementation of different undersampled-based modulation schemes. In addition, experimental results for the bit error rate (BER) performance of the undersampled-based modulation schemes are provided. Moreover, implementation challenges of OCC systems are addressed before our final conclusions are drawn.

II. Types of OCC systems

Based on the IS mechanism, there are mainly two types of digital cameras: those with global shutters (GS) and rolling shutters (RS). In the former, every pixel of IS starts and stops receiving light simultaneously. However, for the latter, pixels are exposed row by row resulting in a time delay between the exposure of the first and the last pixel rows. Different modulation schemes are, therefore, needed if different types of cameras are to be adopted.

In LFR-based OCC systems, there are three main categories of modulation scheme: screen-based modulation, oversampled modulation, and undersampled modulation. More specifically, Fig. 2 illustrates some typical subsets of each category.

1. **Screen-based modulations** — these encode information into image frames that can be read by a camera-based receiver. In general, the two subtypes of screen-based modulations are those that are observable and those unobservable by humans. The first subtype (visible code) encodes the data stream into successive QR code-like 2D visual codes which are then displayed on a screen [6]. The second subtype (invisible code) establishes unobtrusive screen-camera communications by

Fig. 2. Three main categories of modulation schemes for LFR-based OCC systems and their corresponding subcategories.

embedding data in parts of images, and/or particular frames, in both spatial and temporal dimensions. This is done to minimize perceiving visible artifacts in images / animations caused by embedded information [7]. Both subtypes can only support short-range communication (e.g., 10–110 cm [6]).

2. **Oversampled modulations** — similar to most VLC systems, the receiver oversamples the received signal to recover the transmitted data. Polarization-based modulation [4] is one of two oversampled modulations for the LFR camera and it involves two orthogonally polarized lights representing bits "1" and "0" being generated with a frequency of $R_{fc}/2$. Since neither the human eye nor commercial cameras can capture the change of light polarization, no flickering is observed. However, when a polarizer with a certain orientation angle is placed in front of the camera, changes in light polarization are converted into light intensity variations and oversampled by the camera with a sampling rate of R_{fc}. But the received SNR varies with different orientation angles of the polarizer. Therefore, binary color shift keying (BCSK) is proposed in a polarization-based OCC system [4].

The second oversampled modulation is rolling shutter-based modulation where an RS camera captures the incident light row by row with an extremely high scanning rate. Light pulses transmitted at frequencies lower than the scanning rate, and higher than f_{cf}, can, therefore, be captured as dark and bright stripes above the normal image which are unnoticeable by users. Frequency shift keying (FSK) [8] and Manchester coding [9] are typically used to achieve non-flickering data communications using an RS-based camera. However, with such modulation schemes, the entire IS, or, at least, a large section of IS, needs to be illuminated by light which strictly restricts the communication distance d and mobility.

3. **Undersampled modulations** — to facilitate non-flickering communications, f_{fl} must be higher than f_{cf}. However, for LFR cameras with $R_{fc} \leq 60$ fps, their sampling rate is lower than the required f_{cf}. Therefore, undersampled modulation schemes - a type of subcarrier intensity modulation (SIM) - are adopted to transform a baseband signal into a passband signal which is then used for intensity modulation of LEDs with frequency$>f_{cf}$. At the receiver side, a camera continuously captures light emitted by LED(s) with a fixed R_{fc}. The camera can either be an RS or a GS camera. Finally, the original information can be extracted from the brightness of the LED(s) (e.g., ON or OFF state). In undersampled modulation

schemes, there are no requirements for special cameras or R_{fc}, thus, they can support both long-distance and high spectral efficiency communications.

Although all the aforementioned modulation schemes can realize flicker-free OCC, undersampled modulation offers the best potential to increase the total data rate for both short- and long-range scenarios. This is achieved by employing more efficient techniques such as multi-amplitude modulation and multi-wavelength (color) parallel data transmission without the need for high-frame-rate cameras or imaging multiple-input-multiple-output (MIMO). All categories of undersampled modulation schemes shown in Fig. 2 are discussed in the following chapters.

III. Undersampled Modulation

A. *Undersampled frequency shift ON-OFF keying*

Undersampled frequency shift ON-OFF keying (UFSOOK) [10] employs two square-wave subcarriers at frequencies of f_{cA0} and f_{cA1} to represent bits "0" and "1", respectively. Note, that f_{cA0} and f_{cA1} are harmonics of $R_{fc}/2$ (e.g., f_{cA0}=120 Hz, f_{cA1}=105 Hz, at R_{fc} of 30 fps). A frame header (FH) signal with frequency f_{cAFH} (e.g., f_{cAFH}=25 kHz) is also used to represent an intermediate state (i.e., the half on (HO) state) to indicate the start of a data frame. Since the R_{fc} of an LFR camera is lower than both f_{cA0} and f_{cA1}, the camera works in the undersampling mode. Consequently, the undersampled results cannot be used to recover the transmitted data directly. To ensure the correct reception of the original information, aliasing is intentionally introduced.

Fig. 3(a) illustrates an example of a UFSOOK waveform and two possible captured LED states (recorded at the positions of the red-dotted and solid-blue arrows). These arrows represent an LFR camera's two possible sampling positions with the same sampling frequency but different phases. The corresponding binary data bracketed by parentheses are shown above the waveform. As shown in Fig. 3(a), each transmitted baseband signal has a duration of $2/R_{fc}$ and is sampled twice. Due to the special relationship between f_{cA0}, f_{cA1}, f_{cAFH} and R_{fc} [10], when the symbol "1", which contains 7 (odd) square-wave cycles, is sampled, the two captured LED states are different; however for the symbol "0", which contains 8 (even) square-wave cycles, the two captured LED states are identical. Regarding the symbol "FH", two HO states are always captured.

However, the sampled LED states may be inverted because of the different camera sampling phases. From Fig. 3(a), it can be seen that, with the exception of the first FH symbol, the sampled LED states are inverted. Although it appears that this inversion may result in data decoding errors, UFSOOK is able to estimate the original data correctly based on the two neighboring LED states.

For a better understanding of the receiving process, Fig. 3(e) presents images of the three captured LED states — OFF, HO, and ON. Fig. 3(d) also shows a state diagram which illustrates how the information is received in UFSOOK. Note that, more LEDs can be employed to maximize the use of the pixel array of the camera, thus allowing a higher throughput with imaging MIMO.

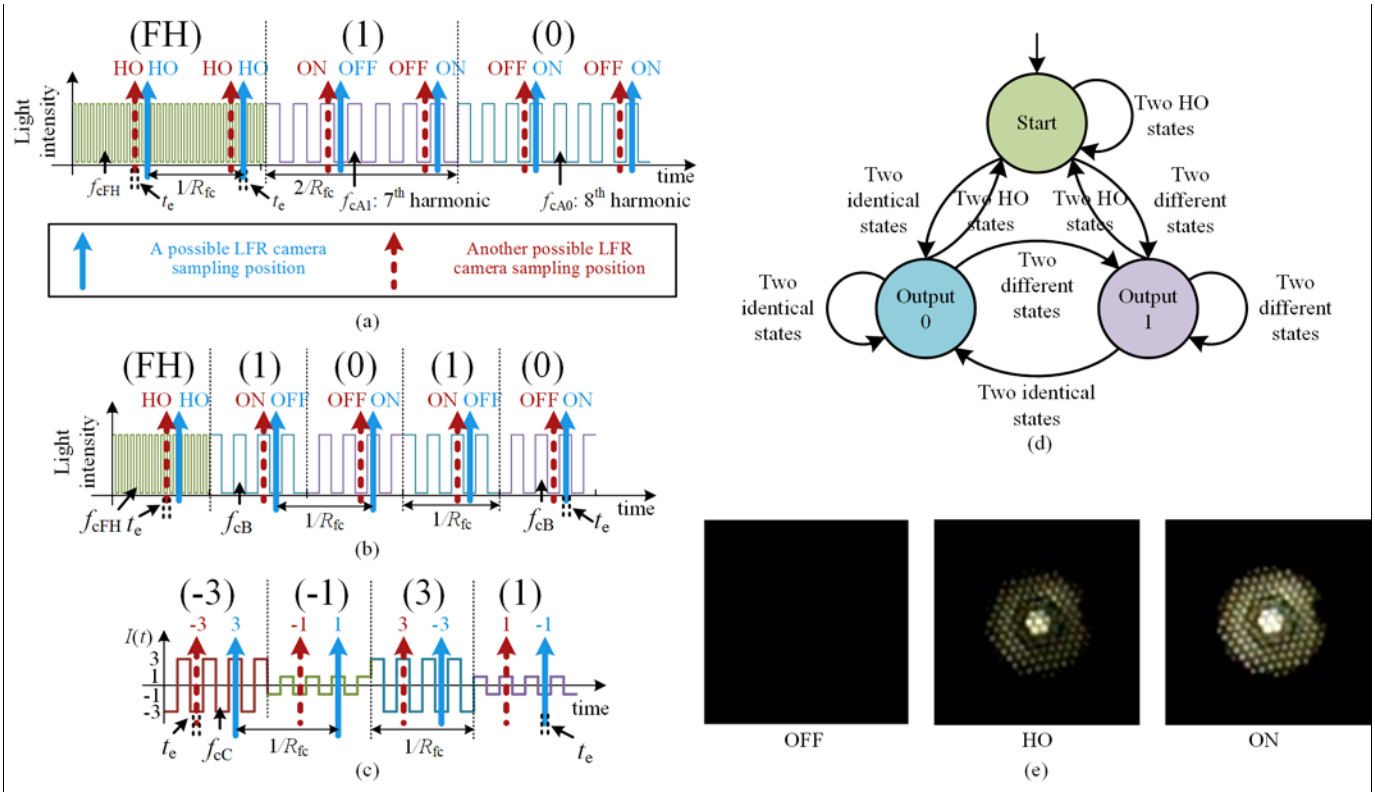

Fig. 3. Two possible sampled results for (a) the same UFSOOK signal (f_{cA0}=4×R_{fc}: 8th order harmonic of $R_{fc}/2$; f_{cA1}=3.5×R_{fc}: 7th order harmonic of $R_{fc}/2$; t_e: exposure time), (b) the same UPSOOK signal (f_{cB}=4×R_{fc}), and (c) the same UPAM signal (AC-coupled, m=4, f_{cC}=4×R_{fc}); (d) a state diagram for the UFSOOK receiver; and (e) photos of the three possible sampled LED states.

Inspired by UFSOOK, a series of undersampled modulation schemes with higher spectral efficiency η_s have been proposed including:

- Undersampled phase shift ON-OFF keying (UPSOOK) [12] - more information is given in Section III.B.
- Undersampled *m*-ary pulse amplitude modulation (UPAM) [11, 13] - more information is given in Section III.C.
- Undersampled modulation with wavelength division multiplexing (WDM) [14] and color shift keying (CSK) - see Section III.D for more information.

All the above-mentioned undersampled modulation schemes have a similar internal structure: a baseband modulation module followed by a square-wave SIM modulator module. Note that, undersampled modulation with WDM generates multiple parallel independent channels where each channel can be modulated by different baseband modulation schemes. The SIM signals are then transmitted via intensity modulated multiple LEDs with different colors (wavelengths). Undersampled modulation with CSK, however, first generates baseband CSK symbols with each symbol being comprised of three dependent parallel channels. The CSK symbols are then fed into the square-wave SIM modulator module, and, finally, transmitted via an RGB LED to produce a non-flickering white light.

B. Undersampled phase shift ON-OFF keying

UPSOOK offers η_s of 1 bit/frame/LED compared with 0.5 bit/frame/LED for UFSOOK by employing phase shift keying [12]. As with UFSOOK, UPSOOK uses two square-wave carriers with the same frequency f_{cB} and amplitude but opposite phases (e.g., θ_{B1}=0°, θ_{B2}=180°) to represent bits "0" and "1". The symbol rate is set to R_{fc} to ensure the transmitter is synchronized with the camera. Consequently, each data symbol is sampled only once by the receiver (i.e., 1 bit/frame/LED). Fig. 3(b) presents an example of the UPSOOK waveform and two possible captured LED states. As shown, each transmitted baseband signal has a duration of $1/R_{fc}$. Similarly, because of the phase uncertainty, the sampled results might be inverted with the exception of the first FH symbol. To eliminate this problem, a framing strategy is proposed in [12]. We will address the dedicated framing strategies for different types of undersampled modulation schemes in detail later.

C. Undersampled m-ary pulse amplitude modulation

Based on the experimental evaluation, an OCC system with an extremely short exposure time (e.g., t_e<1/1000 s) offers an extremely high SNR. Therefore, by adopting multiple amplitude modulation (MAM), higher spectral efficiency η_s can be achieved. UPAM [13], which takes advantage of both UPSOOK and MAM, has a η_s of $\log_2(m)$ bits/frame/LED. Fig. 3(c) presents an example of two possible sampled results captured by a camera when an LED emits a UPAM signal $I(t)$ with a subcarrier frequency of f_{cC} and m=4. Note that, the waveform is AC-coupled. Evidently, due to the phase uncertainty, there are two sampled results sampled by red-dotted and solid-blue arrows: (*i*) the same as $I(i)$ [-3, -1, 3, 1] which is the original data indicated with brackets above $I(t)$; and (*ii*) inversion of the original data. Therefore, an additional phase error detecting process is required which will be outlined later.

Most cameras have a built-in gamma correction feature. This gamma correction nonlinearly encodes all light intensities with a nonlinear profile to compensate for the nonlinearity of human vision. Therefore, nonlinearity will occur if UPAM (multi-amplitude signal, m>2) is transmitted [13]. To compensate for the nonlinear distortion, pre-compensation (PRC) or post-compensation (POC) techniques are adopted [11].

D. Undersampled modulation with WDM or CSK

Generally, a color camera separates the RGB light according to the wavelength of the built-in RGB color filter array. In addition, the RGB LED-based white light lamps, which allow independent modulation of three LED chips, have been widely used. Therefore, the potential to establish a flicker-free WDM or *m*CSK link by using an RGB LED, a color camera and a square-wave SIM is high, thus increasing the data rate compared to the single-chip white LED system.

However, the center wavelength and bandwidth of the color filter of the camera may not match with those of the RGB LEDs perfectly. Thus, for WDM and CSK-based OCC systems, the spectrum overlap between each pair of channels will lead to inter-channel interference (ICI) in the color domain. The crosstalk depends on the transmission spectra of the RGB filters and the wavelength of the incident light. In addition, since a CSK modulator converts parallel data streams into multiple RGB light intensities, the received RGB intensities of the CSK signal experiences distortion from the built-in gamma coding. Therefore, color calibration techniques [15] are needed for both WDM- and CSK-based OCC systems to reduce the ICI. Furthermore, PRC and POC techniques could be adopted to compensate for the nonlinear impairment in these systems.

IV. Framing Strategies To Support Undersampled Modulation Schemes

To solve the problems stated earlier, some solutions have been proposed in the form of framing strategies which are applied before SIM. Fig. 4 outlines an overview of the proposed framing strategies. In detail, Fig. 4(a) lists three potential problems: (*i*) the inversion of all LED states; (*ii*) nonlinear distortion; and (*iii*) ICI. The figure also outlines: the main reasons for these problems; modulation schemes affected by these problems; and possible solutions to these problems. Figs. 4(b)–(*d*) illustrate the proposed framing structures designed specifically to overcome these potential problems. Figs. 4(e)–(g) also depict the concept of a nonlinear compensation scheme.

A. Inversion of all LED states — phase error detection

Inversion of all LED states is a problem, provided there are no phase errors. However, in an undersampled system, the camera - with its two functionalities of sensing the image and undersampling the information - is used to capture the incoming signal. Such a system will experience a phase error problem because of the undersampling process. Consequently,

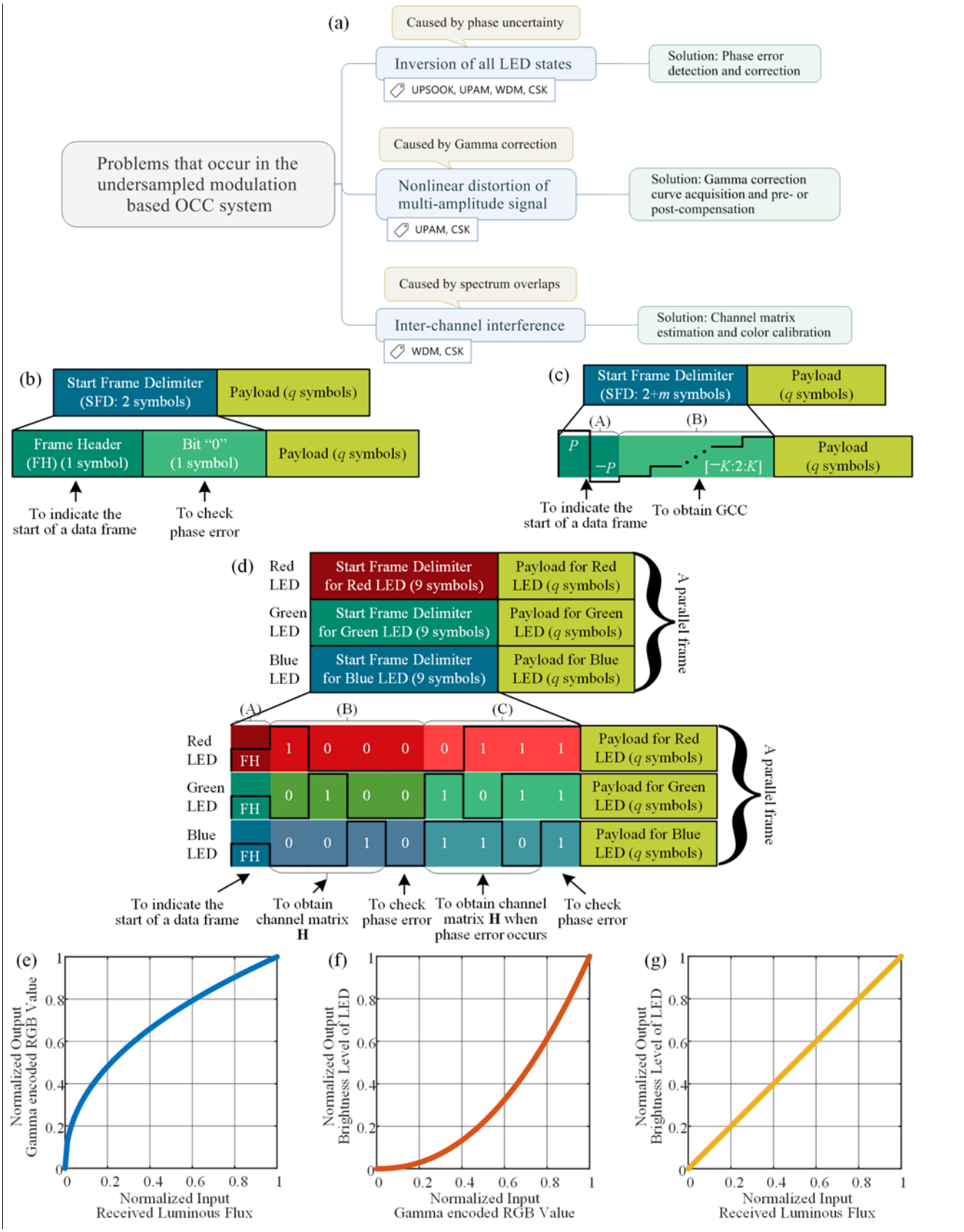

Fig. 4. (a) Problems and solutions for undersampled modulation-based OCC system; (b)–(d): the proposed frame structures for UPSOOK, UPAM (AC coupling) and undersampled modulation with WDM, as well as the function of each part of the SFD; (e) Gamma encoding curve with γ=1/2.2; (f) Gamma encoding compensation curve with γ=2.2; and (g) compensated curve.

a training sequence-based scheme is introduced with the details outlined below.

Fig. 4(b) shows the framing structure for UPSOOK which is composed of two parts: a start frame delimiter (SFD) with two symbols, and a payload with q-symbol, where q is an arbitrary number. As can be seen from Fig. 4(b), the first symbol of the SFD (an FH) will certainly be received as an HO state which indicates the start of a data frame. Regarding the second symbol of the SFD, as we transmit a bit "0" at this position, an OFF state should be received in the second slot of the data frame. Once an ON state is received following the HO state, a phase error is detected. Therefore, an inverse operation of each LED state is required to be performed for this data frame.

B. Nonlinear distortion — compensation techniques

Fig. 4(e) presents a typical gamma correction curve (GCC) with γ=1/2.2. Although gamma encoding is important in photography, this nonlinear distortion is harmful in multi-amplitude communication systems (e.g., UPAM). However, if the GCC data are known by the receiver, the nonlinear distortion can be canceled with an inverse operation (e.g., Fig. 4(f), γ=2.2) of the GCC to ensure a linear proportional relationship between the received optical power (luminous flux) and the brightness level of the image (Fig. 4(g)) of each captured video frame.

To obtain the built-in GCC of the camera, we have added a specially designed SFD before each q-symbol payload (Fig. 4(c)). As shown, SFD consists of two parts. Part A with two symbols: [P, $-P$] (P=m) is designed to indicate the start of a frame and phase error. Due to (P–1) and (–P+1) being the maximum and minimum amplitudes of m-PAM, respectively, there is an uncertainty on the sign of the received UPAM symbol (Fig. 3(e)). On receiving [P, $-P$] or [$-P$, P] the following tasks are performed: (*i*) the data frame is started; and (*ii*) phase error is analyzed to determine if correction is needed.

Part B, with m-symbol, allows the receiver to obtain the GCC information. K (K=m–1) and [–K, 2, K] represent the maximum amplitude and all m-level amplitudes of m-PAM, respectively. Due to the phase error and GCC, there are two possible received signals: (*i*) a waveform where the nonlinear distortion increases with the signal amplitude (i.e., from minimum to maximum); and (*ii*) a waveform where the nonlinear distortion decreases with the signal amplitude (i.e., from maximum to minimum). For both cases, the GCC data could be obtained from this part of SFD. Having obtained the GCC information (refer to [13] for details), the compensation can be performed.

C. Channel matrix estimation

As outlined above, the crosstalk (the mixture of color domain signals) between RGB channels occurs when an RGB chip-based white LED and a color camera are employed. To minimize the performance degradation caused by ICI, color calibration was introduced in [15].

Fig. 4(d) shows an example of a proposed parallel SFD for estimating the 3×3 RGB channel matrix **H**. The detailed SFD structure is demonstrated in the lower part of this figure. As shown, the SFD is comprised of three parts. Part A, with three FH symbols in parallel, identifies the start of a data frame. Parts B and C estimate the channel matrix and check the phase error. The first three parallel symbols in Part B represent a 3×3 identity matrix which shows that RGB LEDs are switched on sequentially. Therefore, with no phase error, the channel matrix can be directly obtained from the corresponding received parallel symbols in Part B. The fourth symbol is used to check for phase errors at the receiver (provided a parallel zero symbol at this position in Part B is received, and there is no phase error and vice versa). Part C, a complement of Part B, is for acquiring the channel matrix **H** in the presence of a phase error. Further details on how the channel matrix is extracted and how the ICI problem is addressed can be found in [14].

V. Practical Experiments

To assess the reliability of the OCC system with the proposed undersampled modulation schemes, BER measurements were performed for both short and long transmission ranges to represent indoor and V2V scenarios, respectively. For the short-range scenario (Fig. 5(a) [11]), two white LEDs (Cree XP-E LED with a lens, an emission semi-angle of 25°) and a Canon 700D RS camera were employed. Parallel UPAM signals can be transmitted simultaneously using two LEDs, while both data streams, with no interference, can be captured using an imaging MIMO based receiver. Since the LED is small in size, dark and bright strips are not observed by the RS camera unless the RS camera is placed a few centimeters away from the LED. Both GS and RS cameras, therefore, can be adopted in our work. The key parameters of the camera were set as an R_{fc} of 50 fps, an exposure time of 1/4000 s, a focal length of 55 mm, an ISO of 100, and video resolution of 960×720. In this work, two modulation orders of 16 and 32, each offering data rates of 200 bps and 250 bps, were used, respectively. For every BER measurement, ~18000 video frames were captured, which is a total of ~1.44×10^5 and ~1.8×10^5 bits of information for the dual LED with 16- and 32-ary PAM, respectively.

In this experiment, the bias voltages for both LEDs were set to 1.5 V, the peak-to-peak voltages of two UPAM signals were changed from 0.3 V to 3 V, and d was set to 1.5 m which is the longest effective distance. Thus, different received illuminance levels (RILs) were achieved by varying the transmitted optical power. Fig. 5(b) [11] illustrates the BER performance against RIL for 16- and 32-ary PAM using two compensation techniques (PRC and POC) with the GCC data extracted from SFD (see Section IV.B). It is apparent that the PRC-based system offers improved performance compared with POC for both values of m. For POC, nonlinear compensation is carried out at the receiver side where the variance of the added noise increases nonlinearly following POC processing. However, for PRC, nonlinear compensation is performed at the transmitter side, showing reduced noise variance. The reliability of the proposed 32-ary UPAM OCC system is also revealed - it can be observed that for an RIL of 19.5 lx, which is a relatively low illumination level, 32-ary PAM with POC could achieve a BER of 2.01×10^{-3}, which is lower than the forward error correction (FEC) limit of 3.8×10^{-3}.

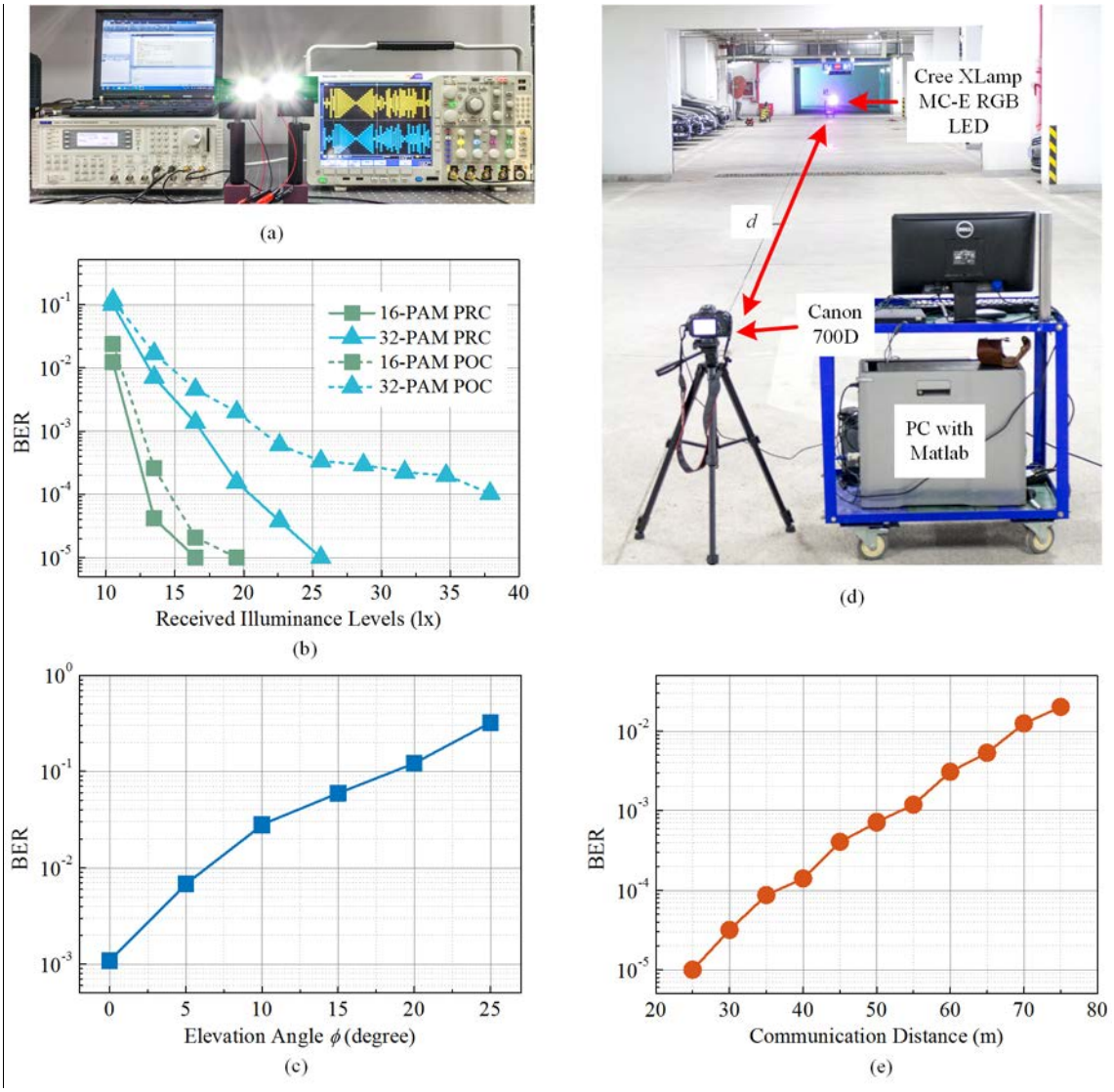

Fig. 5. (a) A photo of the transmitter part of a short-distance UPAM OCC system; (b) dependence of BER performance of the UPAM system with two modulation orders (m=16 and 32) and two compensation techniques (PRC and POC) on received illuminance level; (c) BER performance against the elevation angle ϕ (incident angle θ=0°) for 32-ary UPAM with POC; (d) photograph of a long-distance OCC system with WDM technique; and (e) BER performance vs. communication distance for WDM OCC with UPSOOK using an RGB LED.

To assess the impact of the rotation of the transmitter and the receiver on BER performance, further BER measurements of the 32-ary UPAM OCC system with POC were carried out for a range of transmitter elevation angles ϕ and incident angles θ. For ϕ=0°, the BER remains constant regardless of the receiver's rotation, whereas when θ=0° the BER increases exponentially with ϕ, as shown in Fig. 5(c).

For a long-range WDM OCC system (Fig. 5(d) [14]), we used an RGB LED (Cree XLamp MC-E RGB LED) with a 70° condenser cup and a Canon 700D camera as both the transmitter and receiver, respectively. In the WDM system, using UPSOOK and 3 parallel links, each with a data rate of 50 bps, the total raw data rate achieved was 150 bps.

Fig. 5(e) [14] shows the measured BER performance against the communication distance d for the long-distance outdoor V2V system. Note that, the value of log10(BER) increases linearly as d increases, and when the distance reaches 60 m, the BER increases to 3.1×10^{-3} which is below the FEC limit of 3.8×10^{-3}. Although the total raw data rate is extremely low, it is sufficient for vehicular communications. Higher data rates for outdoor long-distance V2V communications can be achieved by increasing the number of RGB LEDs and adopting imaging MIMO.

VI. Implementation Challenges of OCC Systems

Although OCC systems can be adopted in a range of applications, there are many challenges that need to be addressed in real-world scenarios. For example, the signal loss/error due to inaccurate R_{fc} of a mobile camera, or data errors caused by digital dimming control and movement. Therefore, additional research is required to address these issues and further improve the robustness of the OCC system.

As for the undersampled-based OCC system, the contrast between ON and OFF states of the LED will be significantly

reduced by increasing t_e [8]. To increase the contrast (or SNR) a shorter t_e (e.g., 1/4000 s) is required. However, shorter t_e may lead to underexposed frames, which is harmful from the viewpoint of photography. In practical cases, the clocks for both the transmitter and receiver are only frequency synchronized, with no phase synchronization, therefore, clock jitter or clock skew will be experienced within the system. This may lead to the deterioration of the SNR when the LED state changes during the camera's exposure time, or during the signal reception phase shift. The worst case occurs when the signal edge is located exactly in the middle of t_e when both the received symbols "1" and "0" are in the HO state instead of ON and OFF states. Fortunately, such a case is practically impossible to observe.

To avoid problems due to undersampling issues (e.g., frequency and phase offset between the transmitter and the camera), several approaches can be applied including: (*i*) reducing the carrier frequency, as long as it is higher than the critical flicker frequency of the human eye; (*ii*) introducing the FEC technique to improve the BER performance; and (*iii*) adopting a shorter data frame length to reduce the amount of received signals being affected.

To increase the total data throughput, higher spectral efficiency techniques such as PAM, WDM, and imaging MIMO have been employed, see Table I for the spectral efficiencies of different schemes. Different types of framing strategies were also introduced to overcome problems associated with undersampled modulation schemes. However, the introduction of those techniques will make the OCC system more complicated. New techniques are expected to make the OCC technology simpler and more efficient.

TABLE I. SPECTRAL EFFICIENCY OF DIFFERENT UNDERSAMPLED MODULATION SCHEMES

Modulation schemes	**Spectral efficiency η_s (bits/frame/LED)**
USFOOK	0.5
UPSOOK	1
UPAM	$\log_2(m)$
WDM with UPSOOK	3
*m*CSK with SIM	$\log_2(m)$

VII. CONCLUSIONS

OCC systems exploiting the potential of VLC using smart devices with built-in cameras could be used in many applications, such as indoor positioning systems or intelligent transportation systems. This article gave an overview of a number of modulation schemes for OCC, including undersampled modulations for stable illumination levels, as well as data transmission when employing an LFR camera. In addition, we showed experimental BER results for Canon camera-based OCC systems with different modulation schemes to demonstrate that undersampled modulation schemes with improved spectral efficiency could be adopted in both short- and long-range OCC applications. Finally, the implementation challenges of OCC systems, especially the problems introduced by the undersampling process, were also discussed with some solutions suggested. The spectral efficiencies of different undersampled-based modulation schemes were summarized. We believe that smart devices with more powerful cameras will be used for OCC in a multitude of applications with even higher data rates.

OCC is clearly a promising technology that exploits the widespread use of LED lights and the popularity of smartphones. With the support of undersampled modulation schemes, OCC could enrich life and improve efficiency through a better-connected world.

REFERENCES

[1] Z. Ghassemlooy, P. Luo, and S. Zvanovec, "Optical Camera Communications," in *Optical Wireless Communications*, M. Uysal, C. Capsoni, Z. Ghassemlooy, A. Boucouvalas, and E. Udvary, Eds., ed: Springer, 2016, pp. 547-568.

[2] T. Yamazato, I. Takai, H. Okada, *et al.*, "Image-sensor-based visible light communication for automotive applications," *IEEE Commun. Mag.*, vol. 52, pp. 88-97, 2014.

[3] M. Yoshino, S. Haruyama, and M. Nakagawa, "High-accuracy positioning system using visible LED lights and image sensor," *Proc. RWS*, Orlando, FL, USA, 2008, pp. 439-442.

[4] Z. Yang, Z. Wang, J. Zhang, *et al.*, "Wearables can afford: light-weight indoor positioning with visible light," *Proc. 13th MobiSys*, Florence, Italy, 2015, pp. 317-330.

[5] S. C. Herrmann, "Human EEG responses to 1–100 Hz flicker: resonance phenomena in visual cortex and their potential correlation to cognitive phenomena," *Exp. Brain Res.*, vol. 137, pp. 346-353, 2001.

[6] R. Boubezari, H. L. Minh, Z. Ghassemlooy, *et al.*, "Smartphone Camera Based Visible Light Communication," *J. Lightw. Technol.*, vol. 34, pp. 4121-4127, 2016.

[7] V. Nguyen, Y. Tang, A. Ashok, *et al.*, "High-rate flicker-free screen-camera communication with spatially adaptive embedding," *Proc. 35th INFOCOM*, San Francisco, CA, USA, 2016, pp. 1-9.

[8] N. Rajagopal, P. Lazik, and A. Rowe, "Visual light landmarks for mobile devices," *Proc. 13th ISPN*, Berlin, Germany, 2014, pp. 249-260.

[9] C. Danakis, M. Afgani, G. Povey, *et al.*, "Using a CMOS camera sensor for visible light communication," *Proc. GLOBECOM Wksps*, Anaheim, CA, USA, 2012, pp. 1244-1248.

[10] R. D. Roberts, "Undersampled frequency shift ON-OFF keying (UFSOOK) for camera communications (CamCom)," *Proc. 22nd WOCC*, Chongqing, China, 2013, pp. 645-648.

[11] P. Luo, M. Zhang, Z. Ghassemlooy, *et al.*, "Experimental demonstration of a 1024-QAM optical camera communication system," *IEEE Photon. Technol. Lett.*, vol. 28, pp. 139-142, 2016.

[12] P. Luo, Z. Ghassemlooy, H. L. Minh, *et al.*, "Undersampled phase shift ON-OFF keying for camera communication," *Proc. 6th WCSP*, Hefei, China, 2014, pp. 1-6.

[13] P. Luo, Z. Ghassemlooy, H. L. Minh, *et al.*, "Undersampled-PAM with subcarrier modulation for camera communications," *Proc. 20th OECC*, Shanghai, China, 2015, pp. 1-3.

[14] P. Luo, M. Zhang, Z. Ghassemlooy, *et al.*, "Experimental demonstration of RGB LED-based optical camera communications," *IEEE Photon. J.*, vol. 7, pp. 1-12, 2015.

[15] *IEEE Standard for Local and Metropolitan Area Networks--Part 15.7: Short-Range Wireless Optical Communication Using Visible Light*, Sept. 6 2011.

BIOGRAPHIES

Pengfei Luo (oliver.luo@hisilicon.com) received his Ph.D. degree from Beijing University of Posts and Telecommunications (BUPT), China in 2013. He was a research fellow of Department of Physics and Electrical Engineering, Northumbria University, UK (12/2013-10/2014), and a project assistant in BUPT (11/2014-03/2016). Currently, he is a research engineer at Research Department of HiSilicon, Huawei Technologies Co., Ltd,. His research interests include optical camera communication, indoor positioning technology. More information can be found at http://www.luopf.com

Min Zhang (mzhang@bupt.edu.cn) received his Ph.D. degree in optical

communications from Beijing University of Posts and Telecommunications (BUPT), China. He is now a professor of BUPT. His main research interests include advanced optical communication systems and networks, especially high-speed switching, optical signal processing and optical wireless communications. Prof. Zhang holds 32 China patents. He has authored or co-authored over 300 technical papers in international journals and conferences, and 12 books in the areas of optical communications.

Zabih Ghassemlooy [M'93, SM'02] (z.ghassemlooy@northumbria.ac.uk), B.Sc.(Hons.) (81), MSc (84), and PhD (87). A Research Fellow, City University, U.K (87). Sheffield Hallam University, UK (88-2004), University of Northumbria Newcastle, UK (2004), Chines Academy of Science President's International Fellowship (2016). Published 690 papers (258 journals and 6 books). Research interests optical wireless communications, free space optics, and visible light communications. He is the fellow of the IET, a senior member of IEEE and a member of OSA.

Stanislav Zvanovec [M] (xzvanove@fel.cvut.cz) MSc (02), and PhD (06), full professor and deputy-head of the Department of Electromagnetic Field, Faculty of Electrical Engineering, CTU. Leads Free-space and fiber optics team at CTU, was vice-chair of WG1 of EU COST project IC1101 OPTICWISE, holder of several projects. Published 170 papers, editor of book Visible Light Communications: Theory and Applications. Research interests - wireless optical communications, visible light communications and optical fiber technologies.

Shulan Feng (shulan.feng@hisilicon.com) received her B.S. and M.S. degrees from Harbin Institute of Technology, China in 1997 and 1999, respectively, both in Electrical Engineering. She joined Huawei in 2000 as wireless research engineer. She currently serves as the senior manager of wireless research department of HiSilicon since 2006. Her research interests include cognitive radio, D2D, VLC, 5G and IoT. She has 100+ granted patents and 20+ technical publications.

Philipp Zhang (Chen-Xiong Zhang) [M'86] (philipp.zhang@huawei.com) received the B.S. degree in EE from Shanghai Jiao-Tong University, China, and the M.S. and Ph.D. degrees from KIT, Germany. From 1991 to 1995, he was with SIEMENS Microelectronic Center, Hamburg, Germany. In 1995 he transferred to Interphase Corp., Dallas, Texas. He has worked in start-up companies as CEO/CTO. He has joined Huawei Technologies as Chief Scientist since 2005 and is in charge of corporate research programs and projects.